

Correlation of RTV properties to test data
and its effect on the AXAF mirror performance

Simon C. F. Sheng
Systems Engineering

Oscar Berendsohn
Consultant
Reliability, Materials, System Safety Engineering

Martin R. Schreibman
Space Science Directorate
Hughes Danbury Optical Systems, Inc. (HDOS)
100 Wooster Heights, Danbury, Ct. 06810

Lester M. Cohen

Smithsonian Institution/Astrophysical Observatory
60 Garden Street, Cambridge, MA 02138

ABSTRACT

Using RTV rubber as an interface between mirror elements and their supporting structures during grinding and polishing was proposed for the Advanced X-ray Astrophysics Facility (AXAF) for glass safety concerns. This paper shows that the mirror performance is quite sensitive to the compression modulus of GE RTV-60 which, like all other rubber-like materials, is very difficult to characterize by testing and even more difficult to characterize analytically. Consequently, using representative RTV properties in mirror analyses only produces nominal performance predictions. The envelope of the range of performance has to be determined by using both extremes of the RTV compression modulus.

This paper also presents a comparison between compression moduli generated via testing and that from semi-empirical formulas. The agreement is satisfactory when mean values of the test data are used for comparison and the shape factor is modified to include partially constrained surfaces. The scatter ranges from 7.6% to 23.0% depending upon the way the RTV samples were cast. Using an error of about 16.2%, we were still able to meet the error budget requirements for the Glass Support Fixture (GSF).

1. INTRODUCTION

It was proposed to use RTV rubber as an interface between the AXAF Wolter I conical mirrors and their supporting structures during grinding and polishing primarily for glass safety concerns. Unfortunately, it was found through testing that the compression modulus of RTV is shape dependent and also varied significantly, even when the same procedure of mixing, casting

and curing was followed. Consequently, it was essential to do sensitivity analyses by varying the effective stiffness of the RTV support of the GSF. The sensitivity analyses included random and systematic variation of the RTV compression modulus to explore the worst possibility.

2. SEMI-EMPIRICAL FORMULA FOR COMPRESSION MODULUS

Unlike most metals which are linearly elastic within a fairly large stress range, RTV polymers behave nonlinearly. A typical RTV material has a stress-strain curve with a small slope in the low stress region. This slope keeps increasing until a constant value is reached. Although very similar to the definition of Young's modulus, this slope, referred to as E_c or compression modulus, is dependent on the specimen geometry and cannot be considered as a material constant.

Since rubber-like materials are virtually incompressible, the following two identities apply: $\nu = 0.5$, and $E = 3G$ where " ν " is Poisson's ratio and " G " the shear modulus. Based on these and the additional assumption that the free edge surface of a loaded rubber disk or an infinitely long block will be deformed into a parabolic shape, a formula for E_c can be derived¹

$$E_c = 3G(1 + 2S^2), \quad (1)$$

where " S " is the shape factor defined as

$$S = (\text{one loaded surface})/(\text{free surface}). \quad (2)$$

A material factor " K " was introduced for natural rubber materials and Eq. (1) now takes the following form:

$$E_c = 3G(1 + 2KS^2). \quad (3)$$

This formula had been validated² through a series of tests on RTV-30. By using " K " of 1.0, an agreement on E_c within 15% was established for rectangular specimens with thickness ranging from 0.1 to 0.3 inches and widths varying from 0.47 to 2.0 inches. Two lengths: 0.75 and 1.64 inches were used in that experiment.

For the AXAF GSFs, two RTV pad geometries were used. The one for GSF 1 is 2.5x1.0x0.5 IN³; the other for GSF 2 is 38 IN long with a cross section of 1.0x0.5 IN² in the central portion (35 IN long) and 1.0x0.25 IN² at its ends. Figures of FEM models for these two GSFs are shown in Fig. 1. For the first geometry, the loading head of the INSTRON machine was connected to an aluminum block which covered the entire top surface of the pad, leaving the four sides completely free. For the second geometry, the same aluminum block was used instead of a full length one (35 IN) due to schedule constraints. Therefore, in addition to the loaded surface and free surfaces, the RTV strip contained a third surface of a different nature. The new surfaces, illustrated in

Fig. 2 and referred to as partially constrained surfaces, cannot expand freely outward under loading because of the existence of the surrounding RTV. Here we modify Eq.(2) to reflect the addition of this partially constrained surface.

$$S = (\text{one loaded surface}) / (\text{free surface} + a \times \text{constraint surface}). \quad (4)$$

where "a", varying from 0 for a rigid constraint to 1 for a free surface, is the constraint factor and has to be determined experimentally.

3. SAMPLE PREPARATION AND TESTING PROCEDURE

3.1. Sample preparation

From test results on some early specimens, it was recognized that at low applied stress values (around 10 psi), surface conditions and uniformity of loading were of paramount importance. Consequently, at the later stage of development, the material was cast in a mold with the designated loading surface to the side (top surface is open to air without molding plate) to avoid irregularity in the surfaces. This resulted in a more uniform RTV thickness and a superior finish for the loaded surfaces. Results from specimens molded in both ways are presented below.

3.2. Testing procedure :

During the testing, an aluminum block with a centered spherical depression was used for loading. A steel bearing ball was placed into this depression and the load applied against the ball to obtain a uniform load distribution. The block was then placed on the RTV rubber for loading.

The machine used for loading was an Instron tester. A crosshead speed of 0.02 inch/min and a 20 LBS capacity load cell were used. A strip chart recording of each test was then obtained, from which the compression modulus could be calculated. To establish the error curve for the test assembly (Instron machine and its loading fixtures), a compression test was also done without the RTV specimen. We then used this error curve to correct the deflection curve obtained from tests on RTV so that the deflection due to the apparatus could be excluded.

4. CORRELATION TO TEST DATA

In order to use the most representative stiffness for the RTV pads in subsequent structural analyses, a series of tests had been conducted to determine the typical E_c for RTV-60 pads of the two geometries mentioned above. Here specimens of four different geometries had been used for various practical reasons. Table 1 contains dimensions of these four specimens and their

corresponding test results. The shear modulus "G" was obtained directly from the shear test; the material constant "K" and the constraint factor "a" were derived by using data from compression tests. These constants are needed for calculating E_c by using Eqs.(3) and (4).

Results from test no. 1 on the second geometry (2.5X1.0X.25) and from test no. 4 are considered to be most reliable because the specimen surface which the loading head was acted upon is also one of the molding surfaces. Experience showed that molding RTV this way would minimize the variation in specimen thickness and produce measurements with much less scatter. In fact, the material factor "K" (.7) is obtained by using the test data from the second geometry of test no. 1 where a "G" value of 165 psi from the shear test is used.

Modifying Eq. (2) by adding a constraint factor "a" is necessary because all our tests except test no. 1 involve partially constrained surfaces. A value of 0.77 for "a" is obtained by first calculating shape factors from Eq. (4) and then fitting calculated results from Eqs. (3) to test data from test no. 2. The good agreement found between formula generated E_c 's and those from test no. 3 and 4 with geometries very different from the specimen used in test no. 2 indicates that the constraint factor "a" is probably geometry independent and may be considered as another material constant.

5.SENSITIVITY OF RTV STIFFNESS ON MIRROR PERFORMANCE

5.1.AXAF requirements on grinding :

The primary concern in design of any optic holding GSF for grinding and polishing is the support print-thru of the optic which may be imparted during grinding. Support print-thru is the mirror surface error incurred during grinding or polishing due to the non-uniform supporting of the mirror by the GSF.

For the AXAF application, the print-thru requirements for grinding are:

2.0 μm to 4.0 μm	P/P	for coarse grinding, and
0.2 μm to 0.4 μm	P/P	for fine grinding.

Since the P/P deflection of the optic in its GSF under combined load is closely related to the accumulated print-thru after grinding, it is prudent to adopt a GSF design with the minimum P/P mirror deflection. GSF 2 with a P/P mirror deflection around 0.5 μm is therefore adequate for fine grinding and polishing.

5.1.FEM model

Due to the schedule and cost constraints, it was not feasible to use a custom-made 33 inch long loading head to

produce directly usable E_c data. However, judging from the good correlation established, we had confidence in using the test derived material constants "G", "K" and "a" to calculate E_c through Eqs. (3) and (4). The next step was to reflect the calculated nominal E_c of 1000 psi and G of 165 psi in the finite element model of the GSF 2/mirror assembly and to study the sensitivity of the RTV modulus on mirror deformations.

The model, shown in fig. 1b, was selected for demonstration. Due to symmetry, only a half model is needed. The mirror model shown there is composed of NASTRAN TRIA6 and QUAD8 elements. For each increment of 9 DEG, the model has eight axial elements. This pattern stops at 162 DEG from the top azimuth. From 162 DEG to 180 DEG, a finer mesh is used so that grinding tool loads could be applied to the ID of the optic to determine mirror deformations. This refined mesh is also needed to better represent the deflection of the bottom azimuth of the optic which is the focus of our attention. Each of the 20 full length RTV pads on each stave is modeled as a series of springs with stiffnesses derived from the geometry of the RTV segments with $E_c = 1000$ psi and $G = 165$ psi.

5.2. RTV stiffness on mirror performance

Results from FEM model described above are plotted in Fig. 3 for the bottom azimuth of the mirror. All RTV pads are assumed to have the same nominal E_c . These are curves representing different load cases: gravity, 1500 LB GSF preload, 195 LB of lap load (uniformly distributed or a line load) and different combinations of them. Since the value of E_c may vary within a nominal range of about +8.5%, a study was performed on 3 hypothetical cases including the perceived worst possible situation:

1. Uniform reduction of RTV stiffness by 17% along the entire RTV line of a single stave.
2. Reduction of RTV stiffness by 17% at both ends. Remember that a reduced RTV thickness was deliberately used to double the RTV stiffness at the ends. Losing this feature even partially is a very undesirable situation in terms of mirror performance.
3. A randomly distributed RTV stiffness ranging from -9% to +8% of the nominal stiffness.

The effect of RTV stiffness on mirror performance are summarized in Table 2 for these three cases. Among them, case 2 gives the worst reduction in mirror performance (11.8%). However, it should be emphasized that case 2 is a worst case assumption which is very unlikely to occur in reality.

6. CONCLUSION

The correlation between formula generated compression Moduli

(Ec) and those from four sets of test performed is quite satisfactory. In this procedure, mean values of the test data are used for comparison and shape factors are modified to include constrained surfaces. The scatter ranges from 7.6% to 23.0% depending upon the way RTV samples were cast. When one of the molding surfaces was used as the loading surface, the scatter from mean value was reduced substantially. Since RTV was molded against the actual exterior surface of mirror, the scatter is likely to be about 16.2%. This error, while large, still allows requirements to be met.

Since none of the tests simulates the full length geometry, the Ec of 1000 psi used in the FEM model was not test data but formula generated. Nonetheless, shear modulus G, material constant K and the constraint factor a, which are essential for calculating Ec thru the formula, were determined by the test.

7. REFERENCES

1. A. N. Gent and P. B. Lindley, "Appendix I of The Compression of Bonded Rubber Blocks," Proceedings of Mechanical Engineers, Vol. 173, No. 3, pages 111-122, 1959.
2. Private communication between Itek and Lester M. Cohen of SAO.

Table 1

SUMMARY ON FOUR IN-HOUSE TESTS

TEST NO.	SPECIMEN GEOMETRY (IN ³)	NO. OF SPECIMENS	LOADING HEAD GEOMETRY (IN ²)	Ec ¹ Eq.(4) (PSI)	Ec ² TEST MEAN (PSI)	TEST RANGE /(Ec.max) %
1	2.5X1.X.5	7	2.5X1.0	846	830	15.6
	2.5X1.X.25	3	2.5X1.0	1900	1900	0.0
2	WAFFLE SHAPE with 25 POCKETS (T=.185-.215)	1(25) ⁵	CIRCLE (D=.75)	1638 1602	1613 ³ 1577 ⁴	7.6 9.5
3	33.X1.0XT (T=.498-.537)	1(13)	2.5X1.0	867	879	23.0
4	33.X1.0X.375	1(13)	2.5X1.0	1210	1190	16.2

1 calculated data from Eqs.(3) and (4) with K = .7, a = .77

2 test data from reliability laboratory, HDOS

3 for T = .189, 3 data(B-2,C-2, and D-2)

4 for T = .202, 3 data(B-4,C-4, and D-4)

5 number in the bracket represent the no. of measurements made along the 33 in long RTV strip

Table 2

SENSITIVITY OF RTV STIFFNESS ON MIRROR PERFORMANCE

CASE	P/P MIRROR DEFLECTIONS		PERCENTAGE CHANGE	
	UNIFORM LAP (μ M)	LINE LAP	UNIFORM LAP (%)	LINE LAP
1	.364	.546	5.7	4.7
2	.384	.583	11.5	11.8
3	.357	.544	3.6	4.8
NORMAL	.344	.522	-	-

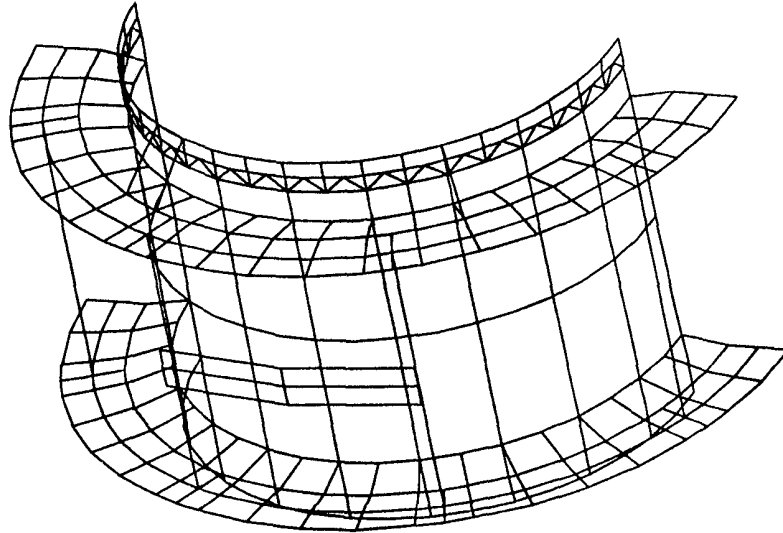


Fig. 1a. GSF 1 for coarse grinding

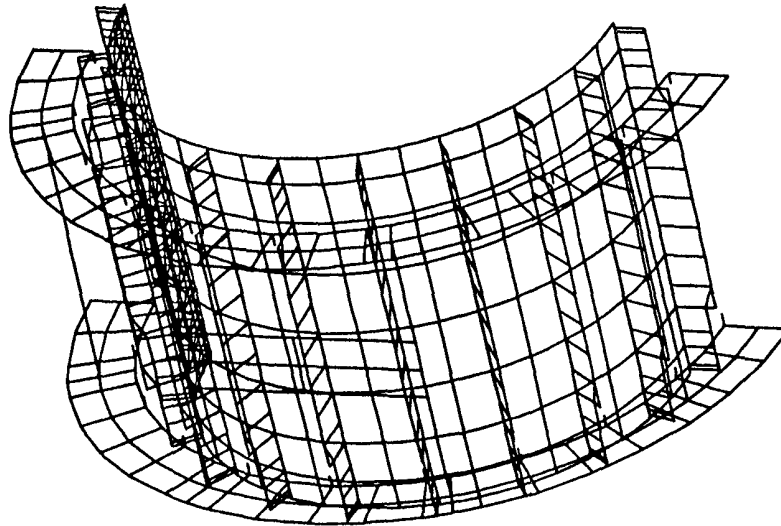


Fig. 1b. GSF 2 for fine grinding and polishing

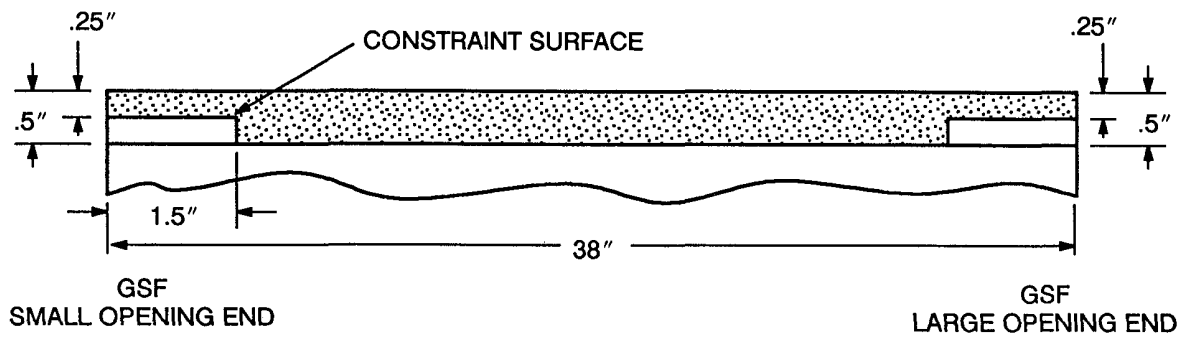


Fig. 2. The RTV geometry of one of the twenty staves for GSF 2

RETROFIT BASELINE
($E_c = 1000\text{psi}$, $G = 165\text{psi}$)

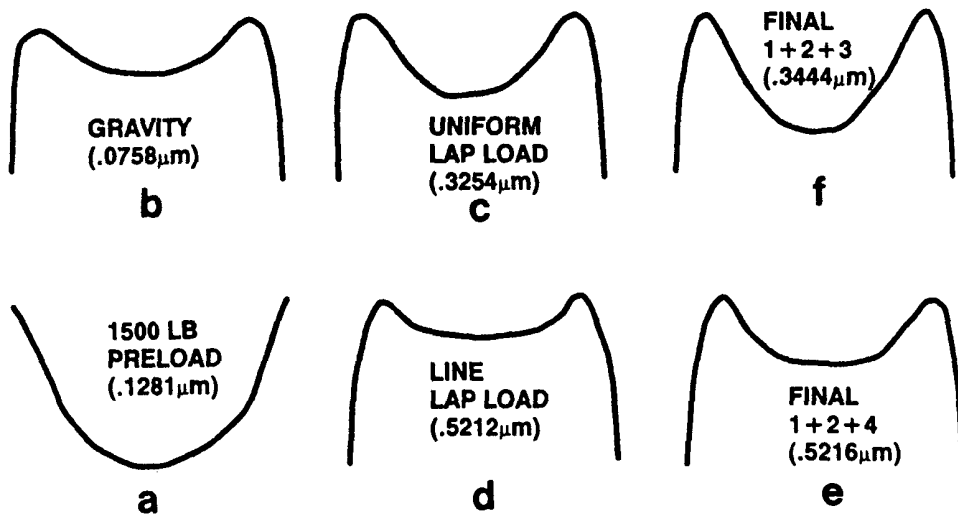


Fig. 3. Deflection curves of the bottom azimuth for different load cases